# Corrugation Effects in Oxygen Surface Trapping at Hyperthermal Energies

A. C. Lavery, C. E. Sosolik, and B. H. Cooper*

*Laboratory of Atomic and Solid State Physics, Cornell University, Ithaca, New York 14853-2501*
(Received 23 August 1999)

We have measured trapping probabilities for $5-600$ eV $O^+$ ions incident on Cu(001) at $45°$ and along the sample normal. These results have been reproduced using classical trajectory simulations. In the simulations, the surface trapping probability $P_S$ is distinguished from the total trapping probability $P_T$. At $45°$, the energy dependence of $P_S$ differs significantly from that of $Na^+$ incident on Cu(001). Trajectory analysis shows that differences between the trapping trends can be attributed to differences in the apparent surface corrugation for these two systems.

Trapping processes are central to a number of thin film growth and surface processing techniques (e.g., sputter, pulsed laser, and ion-assisted deposition and reactive ion etching) that involve hyperthermal energy ion-surface collisions. In these techniques, energy transfer occurs in collisions between surface atoms and various incident ion species over a range of incident energies and angles. The use of energetic beams with control of these parameters can greatly assist in understanding fundamental trapping mechanisms.

When hyperthermal energy ions are incident on a surface, they may scatter from the surface, trap above the top layer of surface atoms, or implant below the surface atoms. For trapping to occur, an incident ion must lose sufficient energy while colliding with the surface atoms that it can no longer escape the attractive potential well, which is typically a couple of eV deep. If the final location of the ion is above the top layer of surface atoms, it is considered surface trapped. We refer to the probability of this occurring as the *surface trapping probability, $P_S$*, to distinguish it from *total trapping probability, $P_T$*, which is the combined probability of trapping above or below the top layer. Below the implantation threshold, $P_S$ and $P_T$ are equivalent. For a given incident ion, the final outcome depends on the incident ion energy and angle, and on the surface species and structure. These factors also determine the surface corrugation seen by the incident ions. In this Letter, we show that surface corrugation plays an important role in determining $P_S$.

We have measured $P_T$, using Auger electron spectroscopy (AES), for $5-600$ eV $O^+$ ions incident on Cu(001)$\langle 100 \rangle$ at $45°$ and at normal incidence. $P_T$ depends very sensitively on the incident ion energy but not on the incident angle. We have successfully reproduced these results using a classical trajectory simulation [1]. There have been previous investigations of hyperthermal O trapping on metal surfaces [2–4]. However, none have looked at the angular dependence of trapping probabilities.

We will also contrast our measurements to those obtained for $Na^+$ incident on Cu(001) [5,6], where a strong dependence of $P_S$ on incident angle was observed. The difference in energy transfer to the surface resulting from the mass difference between O and Na is not sufficient to explain the differences in the trapping trends. Instead, the higher surface corrugation seen by the incident $O^+$ ions is key to explaining the observed differences.

Our measurements were performed in an ultra-high-vacuum system [7,8] with operating pressures below $2 \times 10^{-10}$ Torr. Our beam line produced monoenergetic, hyperthermal energy ion beams which were focused into the 1 mm entrance aperture of a Faraday cup. The Cu(001) single crystal was prepared by standard sputter and anneal cycles. Surface cleanliness and long range order were monitored using AES and low energy electron diffraction (LEED), respectively. A trapping measurement was performed by exposing the sample to the incident O beam for a time, $t$. The resulting oxygen coverage on the sample, $\Theta(\mathbf{r}, t)$, was measured using AES and had a spatial distribution that reflected the shape of the incident ion beam and the incident angle. In the low coverage limit, $\Theta(\mathbf{r}, t)$ is linear with the ion beam dose and is given by $\Theta(\mathbf{r}, t) = P_T(E_i, \theta_i) j(\mathbf{r}) t \cos(\theta_i)$, where $E_i$ and $\theta_i$ are the incident beam energy and angle (relative to the surface normal), and $\mathbf{r}$ is the position on the sample measured from the center of the oxygen coverage. The incident ion current density, $j(\mathbf{r})$, was determined by obtaining a cross-sectional profile of the incident beam current at each $E_i$, using a Faraday cup, and numerically deconvolving to remove effects of the finite size of the Faraday cup aperture [6]. Typical beams were roughly Gaussian in shape with $\sim 0.5$ mm half-widths. To minimize the exposure time of the sample to the incident AES beam, $P_T$ was evaluated at only the center of the O profile on the sample, at $\mathbf{r} = 0$, and is given by $P_T(E_i, \theta_i) = \Theta(0, t) [ j(0) t \cos(\theta_i) ]^{-1}$. $\Theta(0, t)$ was determined by measuring the ratio, $R_{O/Cu}$, of the peak-to-peak heights of the O(503 eV) and Cu(920 eV) Auger signals. $R_{O/Cu}$ was converted to an absolute coverage in monolayers (ML) by depositing $O_2$ up to the known saturation coverage, $\Theta_{sat}$. A $(2 \times 2\sqrt{2})R45$ superstructure is observable using LEED [9] at the known saturation coverage of 0.5 ML, for which $R_{sat} = 0.19$. Thus, $P_T$ is

given by $P_T(E_i, \theta_i) = (\frac{\Theta_{sat}}{R_{sat}})[R_{O/Cu}(0, t)/j(0)t\cos(\theta_i)]$. For $\theta_i = 0°$ and $45°$, and for a range of incident ion energies between 5 and 600 eV, $R_{O/Cu}(0, t)$ was measured for five different beam doses. A linear least squares fit determined $R_{O/Cu}(0, t)[j(0)t\cos(\theta_i)]^{-1}$, from which $P_T$ was evaluated.

Figure 1 shows $P_T(E_i, \theta_i)$ for $\theta_i = 0°$ and $45°$. Within the sensitivity of our measurement, there is little difference between $P_T$ at these two angles. However, there is a significant dependence on $E_i$. $P_T$ decreases by almost a factor of 2 between 5 and 50 eV, while above 50 eV there is a general upward trend. Since typical probing depths of AES are 10–30 Å [10], $R_{O/Cu}$ is sensitive to the presence of O over this entire depth and is not a measure of surface trapping, or $P_S$, alone.

We have performed a full-surface classical trajectory simulation [1] that qualitatively reproduces our data. The simulation uses an O-Cu ion-surface interaction potential that consists of a sum of $[O-Cu]^-$ Hartree-Fock (HF) repulsive pair potentials, calculated using the quantum chemistry package Gaussian 94 [11], and an attractive image term [12,13]. Both $P_S$ and $P_T$ can be found using the simulation and are equivalent until the turn-on of subsurface implantation.

In Fig. 2(a) we plot the results of the simulation for $O^+$ incident at $0°$ and $45°$. The results of the calculation for $P_T$ qualitatively reproduce the data. In particular, $P_T$ and $P_S$ are almost indistinguishable for $\theta_i = 0°$ and $45°$, and there is a significant dependence on $E_i$. Subsurface implantation does not become significant until approximately 40 eV. Thus, the increase of $P_T$ above 50 eV, in both the data and the simulation, can be explained as the increase of subsurface implantation with energy. The quantitative interpretation of the data, above 50 eV, is more complex due

to the depth-dependent sensitivity of the Auger signal [10]. $P_T$ and $P_S$ were also calculated using the well-known Ziegler-Biersack-Littmark and Thomas-Fermi-Moliere potentials [15]. However, these potentials did not reproduce the major trends in the data [12].

Goodstein et al. [5,6] measured $P_S$ for $Na^+$ incident on Cu(001)$\langle 100 \rangle$ at $8°$ and $45°$. They found excellent qualitative agreement between their data and the results of the classical trajectory simulation. In Fig. 2(b) we show the results of the simulation for $Na^+$ incident at $0°$ and $45°$. The most interesting difference between the O and Na results is that, for Na, $P_S$ decreases to near zero at 20–25 eV for the $45°$ case, which is not observed for O. As we will show, this dramatic difference illustrates that $P_S$ is very sensitive to the ion-surface interaction potential. Consequently, measurements of $P_S$ may serve as a sensitive test of calculated interaction potentials.

To understand these results, we must examine the elements that determine when surface trapping occurs. An incident energetic particle can become trapped in the attractive well close to the surface only if it loses sufficient energy upon colliding with the surface. The amount of energy lost depends on the trajectory type, which is a function of the ion-surface interaction potential,



FIG. 1. $P_T(E_i, \theta_i)$ for 5–600 eV $O^+$ incident on Cu(001)$\langle 100 \rangle$ at $\theta_i = 0°$ (circles) and $45°$ (triangles). A typical error bar is shown. The inset shows $P_T$ from 5 to 60 eV.
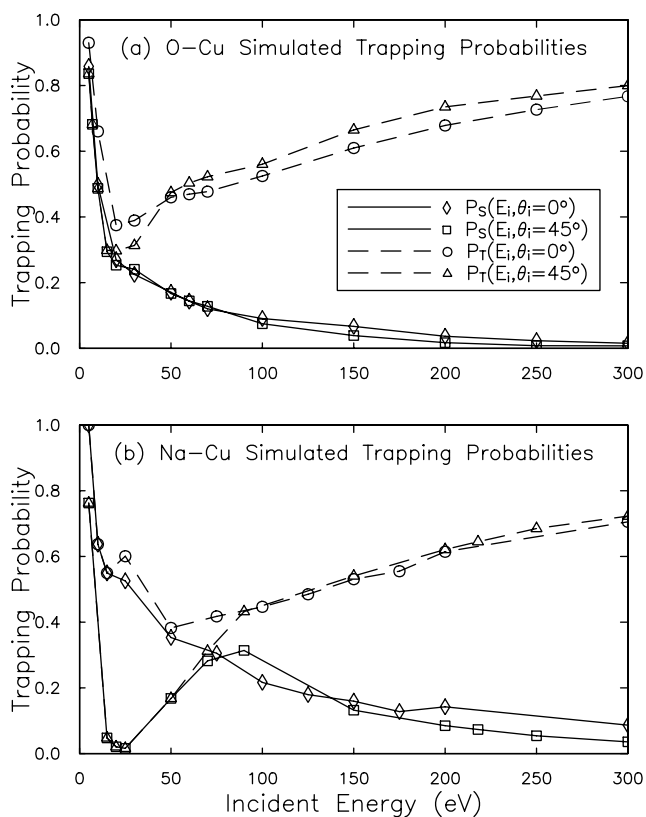


FIG. 2. $P_T(E_i, \theta_i)$ and $P_S(E_i, \theta_i)$ for (a) $O^+$ and (b) $Na^+$ incident on Cu(001). At $45°$, penetration below the top layer turns on at 75 eV for Na and at 40–50 eV for O. At $0°$, subsurface penetration becomes significant only above approximately 50 eV for Na and 40 eV for O.

the impact parameter, and the incident energy and angle. These factors also determine the surface corrugation seen by an incident ion, which increases with $E_i$, and decreases as the scattering becomes more grazing.

Figure 3 compares slices through 5 eV O-Cu and Na-Cu equipotential surfaces along the Cu(001)⟨100⟩ azimuth. Our calculations have shown that the HF pair potential for the O-Cu system is less repulsive than that for the Na-Cu system, resulting in a larger surface corrugation seen by an incident $O^+$ ion, at a given $E_i$ and $\theta_i$, than by an incident $Na^+$ ion.

Detailed analysis [1] has shown that the trajectories that contribute to $P_S$ can be separated into *low-corrugation* (LC) and *high-corrugation* (HC) types. LC trajectories occur when the surface corrugation is low and involve collisions that are inefficient in allowing the incident ions to lose energy. The contribution to $P_S$ from the LC trajectories decreases with increasing $E_i$ since ions undergoing these types of collisions lose energy less effectively with increasing $E_i$. HC trajectories occur when the surface corrugation is larger and involve multiple large-angle collisions that allow the incident ions to lose energy more efficiently. The contribution to $P_S$ from HC trajectories turns on at some $E_i$ and later decreases due to implantation. The differences in $P_S$ between the O-Cu and Na-Cu systems can be explained by examining the energy ranges over which LC and HC trajectory types occur.
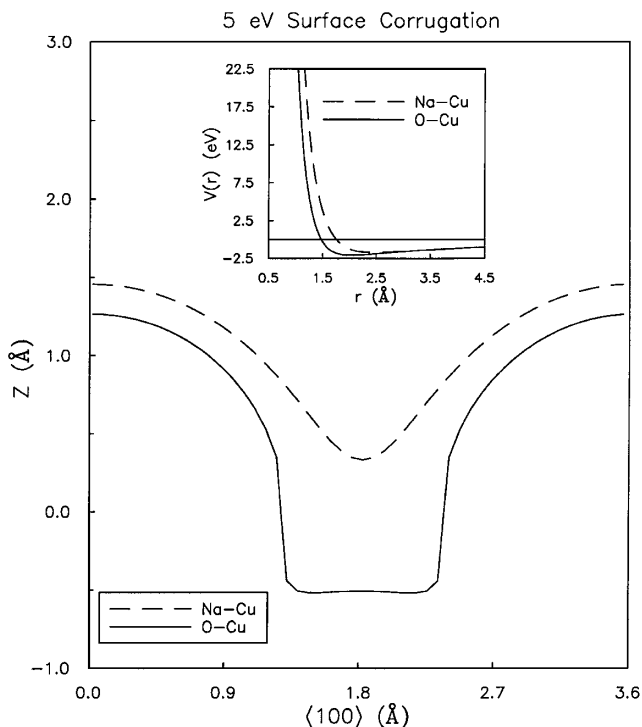
We will concentrate first on explaining the trends in $P_S$ for the Na-Cu system at $\theta_i = 45°$ [Fig. 2(b)]. Below 25 eV, most trajectories are of the LC type, consistent with a relatively low surface corrugation. Figure 4(a) shows a typical 5 eV LC Na trajectory. $P_S$ is high at 5 eV since it is easy for the incident ions to lose sufficient energy to become trapped, even for LC trajectories. As $E_i$ increases from 5 to 25 eV the surface corrugation increases, but it is still not sufficiently high for HC trajectories to occur. As a result, $P_S$ decreases since it becomes harder for incident $Na^+$ ions to lose sufficient energy to become trapped, via the LC trajectories. (Recall that the minimum in $P_S$ for the Na-Cu system at 45° occurs at 25 eV.) Above 25 eV, the surface corrugation increases sufficiently that HC trajectory types begin to dominate. These trajectories result in higher energy losses and $P_S$ increases. Figure 4(b) shows a typical 50 eV HC Na trajectory. As $E_i$ increases above 100 eV, $P_S$ decreases due to implantation.

In contrast to the Na-Cu system, the surface corrugation seen by incident $O^+$ ions at both 0° and 45° is relatively high for all $E_i$. HC trajectories dominate, even at 5 eV, although some LC trajectory types are also present. This is illustrated in Fig. 4 where both the 5 and 50 eV O trajectories are of the HC type. Unlike the Na-Cu system at 45°, there is no clear transition from LC to HC trajectory types at 25 eV, and $P_S$ decreases monotonically.

In summary, the surface corrugation seen by incident $O^+$ ions over the entire energy range is consistently higher than that seen by $Na^+$ incident at 45°, and



FIG. 3.   Cross section through 5 eV O-Cu and Na-Cu equipotential surfaces along the Cu(001)⟨100⟩ azimuth. The inset shows the Na-Cu and O-Cu interaction potentials at an "on-top" site, as a function of distance from the surface.
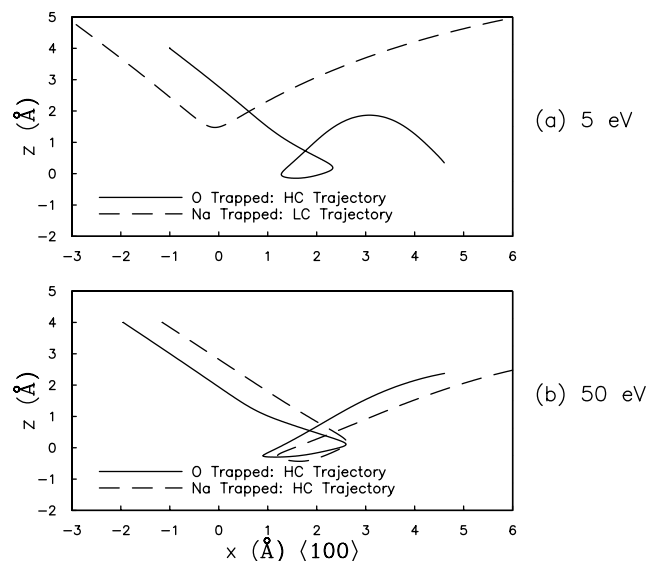


FIG. 4.   Typical trapping trajectories for $Na^+$ (dashed lines) and $O^+$ (solid lines) incident on Cu(001)⟨100⟩ at 45°. (a) $E_i =$ 5 eV and (b) $E_i = 50$ eV. Ions following these trajectories are surface trapped since their total energy is negative. The trajectories shown here are projected onto the scattering plane parallel to the ⟨100⟩ azimuth.
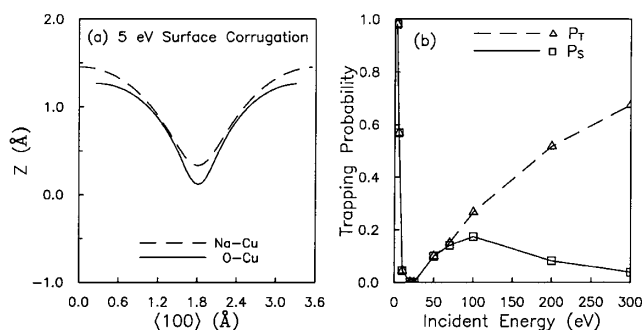
FIG. 5. (a) Cross section through 5 eV equipotential surfaces for $Na^+$ incident on Cu(001) with a lattice constant of 3.61 Å (dashed line) and for $O^+$ incident on an artificial Cu(001) surface with a lattice constant of 3.1 Å (solid line). (b) $P_S$ for $O^+$ incident at 45° on the artificial surface.

surface trapping is dominated by HC trajectory types. Changes in the surface corrugation due to the incident angle have little effect on $P_S$. As $E_i$ increases, $P_S$ decreases due to the turn-on of subsurface implantation and because the incident ions undergoing HC trajectories have increasingly more energy to escape the attractive potential well.

Finally, we turn to the Na-Cu system at $\theta_i = 0°$. The surface corrugation is consistently higher than at 45°, and HC trajectory types occur over the entire energy range. Consequently, $P_S$ for $Na^+$ incident at 0° is qualitatively similar to that for incident $O^+$ at both $\theta_i = 0°$ and 45°, i.e., $P_S$ decreases monotonically with increasing $E_i$.

As we have discussed above, the nonmonotonic trend observed in $P_S$ for $Na^+$ incident at $\theta_i = 45°$ is due to the distinct separation in LC and HC trajectory types at 25 eV. This separation results from a unique combination of the parameters that determine the Na-Cu surface corrugation. To further illustrate the importance of the surface corrugation in surface trapping, we have performed trajectory simulations of $O^+$ incident on an artificial Cu(001) surface, in which the lattice constant has been decreased from 3.61 to 3.1 Å. Reducing the distance between the surface atoms reduces the surface corrugation. The 5 eV equipotential for the artificial O-Cu is shown in Fig. 5(a), together with the 5 eV equipotential for the Na-Cu system with the true lattice constant of 3.61 Å. The surface corrugations are very similar. Figure 5(b) shows $P_S$ and $P_T$ for $O^+$ incident at 45° on the artificial surface. As in the Na-Cu system, there is now a minimum in $P_S$, which drops to zero at 25 eV, clearly illustrating the effects of corrugation on surface trapping.

In this Letter, we have shown that surface trapping probabilities are very sensitive to changes in the surface corrugation seen by the incident ions. In particular, when the surface corrugation is low, changes in the incident angle can have a large effect on $P_S$, as was observed for the Na-Cu system. In contrast, the O-Cu surface corrugation is always sufficiently high that changes in the incident angle no longer have a large affect on $P_S$. The sensitivity of $P_S$ to the surface corrugation could be exploited to test calculated ion-surface interaction potentials. Furthermore, these results may have important implications in thin film growth and surface processing techniques that employ hyperthermal energetic particles [16]. Energy transfer to a surface, without the added complication of contamination, is often accomplished using noble gas beams. However, the ability to tune parameters such as the incident angle and energy to the location of a minimum in $P_S$ may make it possible, with a single beam, to alternate between a regime in which surface deposition can occur and a regime in which energy is transferred to a surface without the occurrence of surface trapping and before the onset of subsurface implantation.

*Recently deceased.

[1] D. M. Goodstein, S. A. Langer, and B. H. Cooper, J. Vac. Sci. Technol. A **6**, 703 (1988).

[2] H. Kang, S. R. Kassi, and J. W. Rabalais, J. Chem. Phys. **88**, 5882 (1988).

[3] H. Akazawa and Y. Murata, J. Chem. Phys. **92**, 5551 (1990).

[4] P. J. van den Hoek and A. W. Kleyn, J. Chem. Phys. **91**, 4318 (1989).

[5] D. M. Goodstein *et al.,* Phys. Rev. Lett. **78**, 3213 (1997).

[6] E. B. Dahl *et al.,* Nucl. Instrum. Methods Phys. Res., Sect. B **125**, 237 (1997).

[7] R. L. McEachern *et al.,* Rev. Sci. Instrum. **59**, 2560 (1988).

[8] D. L. Adler and B. H. Cooper, Rev. Sci. Instrum. **59**, 137 (1988).

[9] M. Wutting, Surf. Sci. **213**, 103 (1989).

[10] D. Briggs and M. P. Seah, *Practical Surface Analysis* (John Wiley and Sons, Inc., New York, 1990).

[11] M. J. Frisch *et al.,* GAUSSIAN 94 (Gaussian, Inc., Pittsburgh, 1994).

[12] A. C. Lavery, Ph.D. thesis, Cornell University, 1999.

[13] The trajectory simulation does not incorporate effects due to charge transfer processes. However, the incident $O^+$ ions will be converted to $O^-$ close to the surface [14]. In addition, our calculations have shown that the differences between the $[O\text{-}Cu]^-$, $[O\text{-}Cu]^0$, and $[O\text{-}Cu]^+$ pair potentials are small.

[14] A. C. Lavery *et al.,* Phys. Rev. B (to be published).

[15] S. H. Overbury and D. R. Huntley, Phys. Rev. B **32**, 6278 (1985).

[16] J. Jacobsen, B. H. Cooper, and J. P. Sethna, Phys. Rev. B **58**, 15847 (1998).